Efficient Iterative Design Method for Cosine-Modulated QMF Banks

Hua Xu, *Stuudent Member, IEEE*, Wu-Sheng Lu, *Senior Member, IEEE*, and Andreas Antoniou, *Fellow, IEEE*

***Abstract*—An iterative algorithm for the design of multichannel cosine-modulated quadrature mirror-image filter (QMF) banks with near-perfect reconstruction is proposed. The objective function is formulated as a quadratic function in each step whose minimum point can be obtained using a closed-form solution. This approach has high design efficiency and leads to filter banks with high stopband attenuation and low aliasing and amplitude distortions. The proposed approach is then extended to the design of multichannel cosine-modulated QMF banks with low reconstruction delays, which are often required, especially in real-time applications. Several design examples are included to demonstrate the proposed algorithms, and some comparisons are made with existing designs.**

I. Introduction

MULTIRATE signal processing and filter bank systems have found many applications in areas such as speech and image coding [1]–[5] during the past 20 years, and extensive research has been carried out in the analysis and design of filter banks. The research effort was first focused on one-dimensional (1-D) two-channel filter banks [6]–[10], and later, it was extended to multichannel filter banks [11]–[19]. Among the various multichannel filter banks, the cosine-modulated QMF bank has two advantages:

1) The analysis and synthesis filters are all obtained from a prototype filter, and consequently, only the prototype filter needs to be designed. This results in high design efficiency.
2) There are polyphase structures that make the implementation of the filter bank very efficient.

Multichannel cosine-modulated QMF banks can be categorized into two groups: near-perfect and perfect-reconstruction banks.

To date, many approaches have been proposed for the design of multichannel cosine-modulated QMF banks. In [12]–[17], filter banks with near-perfect reconstruction are considered. In [18] and [19], methods for the design of perfect-reconstruction filter banks are proposed. With the exception of the method in [15], these approaches use standard constrained or unconstrained optimization techniques to obtain the design, which, in general, are quite time consuming.

In this paper, we propose a new optimization algorithm in which, instead of being minimized directly, the objective function is converted into a quadratic function of the filter coefficients whose minimum point can be obtained analytically. Then, a linear formula is adopted to update the coefficient vector, and the procedure is repeated until a termination criterion is met. The approach reduces the computational complexity significantly and leads to filter banks with high stopband attenuation and low aliasing and amplitude distortions.

Most cosine-modulated QMF banks investigated so far have reconstruction delays of $N-1$, where N is the filter length. When the filter length is high, which is very common in multichannel filter bank designs, the reconstruction delay will be long, which is undesirable for real-time applications. In [17], some preliminary results have been given through a design example on low-delay cosine-modulated QMF banks. In [20], a class of cosine-modulated filter banks was proposed whose reconstruction delay can take several values. In this paper, a general cosine-modulated QMF bank is considered in which no constraint is imposed on the filter length N and the reconstruction delay k_d. By letting $k_d < N-1$, a low-delay cosine-modulated QMF bank can be obtained. The iterative algorithm proposed is then applied for the design of low-delay filter banks with near-perfect reconstruction.

The organization of the paper is as follows: In Section II, the structure of multichannel cosine-modulated QMF banks is first reviewed, and the objective function is formed. Then, the iterative approach for minimizing the objective function is developed. In Section III, a general cosine-modulated QMF bank is proposed, and an iterative approach similar to that in Section II is applied to design low-delay cosine-modulated QMF banks. Section IV includes several design examples that demonstrate the proposed algorithms and provides performance comparisons with several other existing designs.

II. Conventional Cosine-Modulated QMF Bank

A. Review

In the M-channel filter bank shown in Fig. 1, the reconstructed signal is given by [14]

$$\hat{X}(z) = \frac{1}{M}\sum_{k=0}^{M-1} F_k(z)\sum_{l=0}^{M-1} H_k(W_M^l z)X(W_M^l z) = \sum_{l=0}^{M-1} T_l(z)X(W_M^l z) \tag{1}$$

Manuscript received October 11, 1994; revised December 11, 1995. This work was supported by Micronet, the Networks of Centres of Excellence Program, and the Natural Science and Engineering Council of Canada. The associate editor coordinating the review of this paper and approving it for publication was Dr. Troung Q. Nguyen.

The authors are with the Department of Electrical and Computer Engineering, University of Victoria, Victoria, BC, Canada V8W 3P6.

Publisher Item Identifier S 1053-587X(96)04533-3.

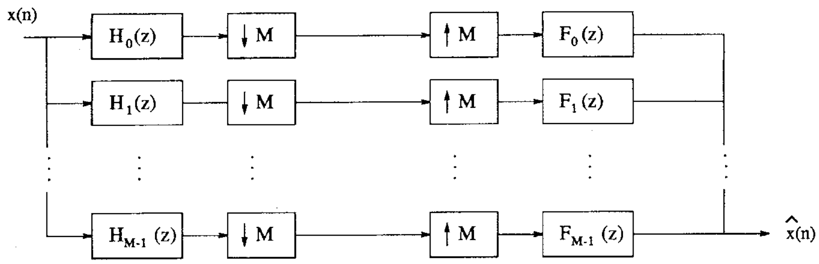

Fig. 1. M-channel filter bank.

where

$$W_M = e^{-2\pi j/M}$$
$$T_l(z) = \frac{1}{M}\sum_{k=0}^{M-1} F_k(z)H_k(W_M^l z).$$

In order to cancel aliasing and achieve perfect reconstruction, it is required that

$$T_l(z) = 0 \qquad \text{for } l = 1, 2, \cdots, M-1 \tag{2a}$$
$$T_0(z) = z^{-k_d} \qquad k_d \text{ is an integer.} \tag{2b}$$

In a cosine-modulated QMF bank, the transfer functions of the analysis and synthesis filters $H_k(z)$ and $F_k(z)$ for $k = 0, 1, \cdots, M-1$, respectively, are obtained by modulating the transfer function $P(z)$ of a prototype linear-phase lowpass FIR filter P with bandwidth $\pi/(2M)$, i.e.

$$H_k(z) = a_k c_k P(zW_{2M}^{(k+1/2)}) + a_k^* c_k^* P(zW_{2M}^{-(k+1/2)}) \tag{3a}$$
$$F_k(z) = a_k^* c_k P(zW_{2M}^{(k+1/2)}) + a_k c_k^* P(zW_{2M}^{-(k+1/2)}) \tag{3b}$$

for $0 \leq k \leq M-1$, where $a_k = e^{j\theta_k}, c_k = W_{2M}^{(k+1/2)(N-1)/2}, W_{2M} = e^{-j\pi/M}$, and N is the length of filter P. The superscript * denotes the complex conjugate operation. It follows that the impulse responses of the analysis and synthesis filters H_k and F_k are given by

$$h_k(n) = 2p(n)\cos\left[(2k+1)\frac{\pi}{2M}\left(n - \frac{N-1}{2}\right) + \theta_k\right] \tag{4a}$$
$$f_k(n) = 2p(n)\cos\left[(2k+1)\frac{\pi}{2M}\left(n - \frac{N-1}{2}\right) - \theta_k\right] \tag{4b}$$

for $0 \leq n \leq N-1$ and $0 \leq k \leq M-1$, respectively, and $p(n)$ is the impulse response of the prototype filter P. From (3) and (4), the analysis and synthesis filters are related by

$$f_k(n) = h_k(N-1-n)$$
$$F_k(z) = z^{-(N-1)}\tilde{H}_k(z)$$

where $\tilde{H}_k(z) = H_k^*(z^{-1})$, for $k = 0, \cdots, M-1$. As shown in [14], θ_k can be chosen as

$$\theta_{k+1} = \theta_k \pm \frac{\pi}{2} \qquad \text{for } 0 \leq k < M-1 \tag{5}$$

in order to cancel significant aliasing terms. In order to assure a relatively flat overall amplitude response, it is required that

$$\theta_0 = \pm\left(\frac{\pi}{4} + \frac{l\pi}{2}\right) \tag{6a}$$
$$\theta_{M-1} = \pm\left(\frac{\pi}{4} + \frac{m\pi}{2}\right) \tag{6b}$$

where l and m are integers. A good choice of θ_k that satisfies (5) and (6) is

$$\theta_k = (2k+1)\pi/4 \qquad \text{for } 0 \leq k \leq M-1. \tag{7}$$

Under these circumstances, the overall transfer function becomes

$$\begin{aligned} T_0(z) &= \frac{1}{M}\sum_{k=0}^{M-1} H_k(z)F_k(z) \\ &= \frac{z^{-(N-1)}}{M}\sum_{k=0}^{M-1} H_k(z)\tilde{H}_k(z) \end{aligned}$$

and hence

$$T_0(e^{j\omega}) = \frac{e^{-j\omega(N-1)}}{M}\sum_{k=0}^{M-1} |H_k(e^{j\omega})|^2. \tag{8}$$

Note that (8) is derived on the basis of the assumption in (2a), and hence, it represents the overall frequency response of the filter bank exactly only if the aliasing components are exactly zero. From (8), it follows that the filter bank has a linear-phase response, which leads to a reconstructed signal with no phase distortion. If the amplitude distortion introduced by the filter bank is eliminated as well, i.e.

$$\sum_{k=0}^{M-1} |H_k(e^{j\omega})|^2 = 1 \tag{9}$$

for $0 \leq \omega \leq \pi$, then perfect reconstruction will be achieved, and the reconstruction delay will be $N-1$ sampling periods.

B. New Iterative Method

It can be shown that $|T_0(e^{j\omega})|$ has a period of π/M, and if the prototype filter P has a large stopband attenuation, (8) gives

$$\begin{aligned} T_0(e^{j\omega}) \approx \frac{e^{-j\omega(N-1)}}{M}&[|P(e^{j(\omega - k\pi/M - \pi/2M)})|^2 \\ &+ |P(e^{j(\omega-(k+1)\pi/M - \pi/2M)})|^2] \end{aligned} \tag{10}$$

for ω in the range of $(k+\frac{1}{2})\pi/M \le \omega \le (k+\frac{3}{2})\pi/M$ [14]. Note that the quantity in the square brackets of (10) is a frequency-shifted version of $|P(e^{j\omega})|^2 + |P(e^{j(\omega-(\pi/M))})|^2$, and, therefore, if this term can be made constant over $[0, \pi/M]$, then $|T_0(e^{j\omega})|$ will be constant for all frequencies, that is, amplitude distortion is eliminated. Hence, the design problem can be reduced to the problem of minimizing the objective function

$$E = E_1 + \alpha E_2 \tag{11a}$$

where

$$E_1 = \int_0^{\pi/M} [|P(e^{j\omega})|^2 + |P(e^{j(\omega-\pi/M)})|^2 - 1]^2 \, d\omega \tag{11b}$$

deals with the amplitude distortion of the overall transfer function $T_0(z)$

$$E_2 = \int_{\omega_s}^{\pi} |P(e^{j\omega})|^2 \, d\omega \tag{11c}$$

deals with the stopband attenuation of the prototype filter P, where $\omega_s = \pi/(2M) + \varepsilon$, and ε is a positive constant that depends on the required transition width. Parameter α is a positive weight. Since filter P is a linear-phase lowpass filter with a symmetrical impulse response, when N is even, its frequency response can be expressed as [21]

$$P(e^{j\omega}) = M_p(\omega) e^{-j\omega(N-1)/2} \tag{12a}$$

$$M_p(\omega) = 2\boldsymbol{p}^T \boldsymbol{c}(\omega) \tag{12b}$$

where $\boldsymbol{c}(\omega) = [\cos(N-1)\omega/2 \cdots \cos\omega/2]^T$, and $\boldsymbol{p} = [p(0)\, p(1) \cdots p((N/2)-1)]^T$. Therefore, E_1 and E_2 in (11) can be rewritten as

$$E_1 = \int_0^{\pi/M} \left[M_p^2(\omega) + M_p^2\left(\omega - \frac{\pi}{M}\right) - 1\right]^2 d\omega$$

$$E_2 = \int_{\omega_s}^{\pi} M_p^2(\omega)\, d\omega.$$

Minimizing E in (11a) using a standard optimization method tends to be time consuming since the objective function is highly nonlinear. Instead of minimizing function E directly, we adopt an iterative procedure in which the objective function in (11a) is modified to

$$E' = E_1' + \alpha E_2' \tag{13a}$$

where

$$E_1' = \sum_{0\le\omega\le\pi/M} \left[M_p(\omega)\cdot M_q(\omega) + M_p\left(\omega - \frac{\pi}{M}\right) \cdot M_q\left(\omega - \frac{\pi}{M}\right) - 1\right]^2 \tag{13b}$$

$$\begin{aligned} E_2' &= \int_{\omega_s}^{\pi} M_q^2(\omega)\, d\omega \\ &= 4\boldsymbol{q}^T \left[\int_{\omega_s}^{\pi} \boldsymbol{c}(\omega)\boldsymbol{c}^T(\omega)\, d\omega\right] \boldsymbol{q} \\ &= \boldsymbol{q}^T \boldsymbol{U}_s \boldsymbol{q} \end{aligned} \tag{13c}$$

and

$$Q(e^{j\omega}) = M_q(\omega) e^{-j\omega(N-1)/2}$$

$$M_q(\omega) = 2\boldsymbol{q}^T \boldsymbol{c}(\omega)$$

with $\boldsymbol{q} = [q(0)\, q(1) \cdots q(N/2-1)]^T$. $Q(e^{j\omega})$ is the frequency response of a lowpass linear-phase FIR filter Q with a passband width $\pi/(2M)$.

At the beginning of the iterative procedure, filter P is first designed using one of the conventional methods such as the window method, Remez exchange algorithm [21], etc. The summation in (13b) is carried out over a set of sampling points $\boldsymbol{\Omega}_p = \{\omega_{p1} = 0, \omega_{p2}, \cdots, \omega_{pk} = \pi/M\}$. Then, E' in (13a) can be formulated as a quadratic function of $\boldsymbol{q}$ given by

$$E' = (\boldsymbol{U}\boldsymbol{q} - \boldsymbol{d})^T(\boldsymbol{U}\boldsymbol{q} - \boldsymbol{d}) + \alpha(\boldsymbol{q}^T \boldsymbol{U_s} \boldsymbol{q}) \tag{14}$$

where $\boldsymbol{d}$ is a column vector with each entry being a 1, and

$$\boldsymbol{U} = \boldsymbol{H}(\boldsymbol{\Omega}_p)\boldsymbol{U_t}(\boldsymbol{\Omega}_p) + \boldsymbol{H}\left(\boldsymbol{\Omega}_p - \frac{\pi}{M}\right)\boldsymbol{U_t}\left(\boldsymbol{\Omega}_p - \frac{\pi}{M}\right) \tag{15a}$$

$$\boldsymbol{H}(\boldsymbol{\Omega}_p) = \mathrm{diag}[M_p(\omega_{p1}), M_p(\omega_{p2}), \cdots, M_p(\omega_{pk})] \tag{15b}$$

$$\boldsymbol{U_t}(\boldsymbol{\Omega}_p) = 2\begin{bmatrix} \cos(N-1)\omega_{p1}/2 & \cdots & \cos\omega_{p1}/2 \\ \cos(N-1)\omega_{p2}/2 & \cdots & \cos\omega_{p2}/2 \\ \vdots & & \vdots \\ \cos(N-1)\omega_{pk}/2 & \cdots & \cos\omega_{pk}/2 \end{bmatrix}. \tag{15c}$$

The (i,j)th entry of $\boldsymbol{U}_s$ is given by

$$\begin{aligned} u_{ij}^{(s)} &= 4\int_{\omega_s}^{\pi} \cos\left[\left(i - 1 - \frac{N-1}{2}\right)\omega\right] \cdot \cos\left[\left(j - 1 - \frac{N-1}{2}\right)\omega\right] d\omega \\ &= 4 \cdot \begin{cases} \dfrac{\pi - \omega_s}{2} - \dfrac{\sin[(2i-N-1)\omega_s]}{2(2i-N-1)} & \text{for } i = j \\ \dfrac{\sin[(i-j)\omega_s]}{2(j-i)} - \dfrac{\sin[(i+j-N-1)\omega_s]}{2(i+j-N-1)} & \text{for } i \ne j \end{cases} \end{aligned} \tag{15d}$$

for $i, j = 1, 2, \cdots, N/2$.

Since $\boldsymbol{U}^T\boldsymbol{U} + \alpha\boldsymbol{U_s}$ is positive definite, E' has a global minimum point at

$$\boldsymbol{q} = (\boldsymbol{U}^T\boldsymbol{U} + \alpha\boldsymbol{U_s})^{-1} \cdot (\boldsymbol{U}^T\boldsymbol{d}). \tag{16}$$

Having obtained $\boldsymbol{q}$, a linear formula is used to update $\boldsymbol{p}$ as

$$\boldsymbol{p} := (1-\tau)\boldsymbol{p} + \tau\boldsymbol{q} \tag{17}$$

where τ, $0 < \tau < 1$, is a smoothing parameter. The above process is repeated until $\|\boldsymbol{p} - \boldsymbol{q}\|_2$ is less than a specified tolerance.

The iterative algorithm can now be summarized in terms of the following steps:

Algorithm 1

Step 1: Use a conventional method to design a linear-phase, lowpass, FIR filter of length N with a bandwidth of $\pi/(2M)$. Then, use the coefficient vector of the filter obtained to initialize $\boldsymbol{p}$.

Step 2: Use (15d) to compute matrix $\boldsymbol{U}_s$.

Step 3: Form matrix $\boldsymbol{U}$ and vector $\boldsymbol{q}$ by using (15a) and (16), respectively.

Step 4: If $\|\boldsymbol{p}-\boldsymbol{q}\|_2<\epsilon$, where ϵ is a prescribed tolerance, output $\boldsymbol{p}$ as the design result and stop; otherwise, update $\boldsymbol{p}$ using (17) with τ in the range $0<\tau<1$, say, $\tau=0.5$, and repeat from Step 3.

In the above analysis, N is assumed to be even. If N is odd, the frequency response of P can still be expressed as in (12a) with

$$M_p(\omega)=\boldsymbol{p}^T\boldsymbol{c}(\omega)$$

where

$$\begin{aligned}\boldsymbol{c}(\omega)&=[\cos(N-1)\omega/2\ \cos(N-3)\omega/2\cdots\cos\omega 1]^T\\ \boldsymbol{p}&=[2p(0)\ 2p(1)\cdots 2p((N-3)/2)\ p((N-1)/2)]^T\end{aligned}$$

and Algorithm 1 is valid if (15c) and (15d) are modified as

$$\boldsymbol{U_t}(\boldsymbol{\Omega}_p)=\begin{bmatrix}\cos(N-1)\omega_{p1}/2 & \cdots & \cos\omega_{p1} & 1\\ \cos(N-1)\omega_{p2}/2 & \cdots & \cos\omega_{p2} & 1\\ \vdots & & & \vdots\\ \cos(N-1)\omega_{pk}/2 & \cdots & \cos\omega_{pk} & 1\end{bmatrix} \tag{18a}$$

$$u_{ij}^{(s)}=\begin{cases}\pi-\omega_s & \text{for } i=j=\dfrac{N+1}{2}\\ \dfrac{\pi-\omega_s}{2}-\dfrac{\sin[(2i-N-1)\omega_s]}{2(2i-N-1)} & \text{for } i=j<\dfrac{N+1}{2}\\ \dfrac{\sin[(i-j)\omega_s]}{2(j-i)}-\dfrac{\sin[(i+j-N-1)\omega_s]}{2(i+j-N-1)} & \text{for } i\neq j\end{cases} \tag{18b}$$

for $i,j=1,2,\cdots,(N+1)/2$, respectively.

Although a rigorous proof of the algorithm's convergence is not available at this time, the algorithm was found to always converge in a large set of designs when the initial point is obtained as in Step 1. Moreover, the algorithm converges faster if τ is chosen to be in the vicinity of 0.5.

III. Low-Delay Cosine-Modulated QMF Bank

A. A General Cosine-Modulated QMF Bank

The reconstruction delay of the cosine-modulated QMF bank described in Section II (referred to as the conventional cosine-modulated QMF bank henceforth) is $N-1$ sampling periods, where N is the filter length. When the number of channels M increases in a filter bank, the bandwidth of each filter decreases, and as a result, high-order filters are required to achieve the narrow passband. Consequently, the filter banks designed have long reconstruction delays, which are highly undesirable in some applications. In this section, we extend the method of Section II to the design of low-delay cosine-modulated QMF banks.

Consider a prototype FIR lowpass filter P_L of length N with an *asymmetrical* impulse response, a bandwidth of $\pi/(2M)$, and a phase response that is approximately linear. Its frequency response can be expressed as

$$P_L(e^{j\omega})\approx|P_L(e^{j\omega})|e^{-j\omega k_d/2} \tag{19}$$

and hence, the group delay of the filter is $k_d/2$, where $k_d\le N-1$. The transfer functions of the analysis and synthesis filters $H_k(z)$ and $F_k(z)$ are related to the transfer function $P_L(z)$ of the prototype lowpass filter P_L as

$$H_k(z)=e^{j\phi_k}P_L(W_{2M}^{(k+1/2)}z)+e^{-j\phi_k}P_L(W_{2M}^{-(k+1/2)}z) \tag{20a}$$

$$F_k(z)=e^{j\psi_k}P_L(W_{2M}^{(k+1/2)}z)+e^{-j\psi_k}P_L(W_{2M}^{-(k+1/2)}z) \tag{20b}$$

for $0\le k\le M-1$, where

$$\begin{aligned}\phi_k&=(M-k_d)(2k+1)\pi/(4M)\\ \psi_k&=(-M-k_d)(2k+1)\pi/(4M).\end{aligned}$$

From (1) and (20), the aliasing terms in the reconstructed signal can be written as

$$\begin{aligned}T_l(z)=\frac{1}{M}\sum_{k=0}^{M-1}&e^{j(\phi_k+\psi_k)}P_L(W_{2M}^{(2l+k+1/2)}z)P_L(W_{2M}^{(k+1/2)}z)\\ &+e^{j(\phi_k-\psi_k)}P_L(W_{2M}^{(2l+k+1/2)}z)P_L(W_{2M}^{-(k+1/2)}z)\\ &+e^{-j(\phi_k-\psi_k)}P_L(W_{2M}^{(2l-k-1/2)}z)P_L(W_{2M}^{(k+1/2)}z)\\ &+e^{-j(\phi_k+\psi_k)}P_L(W_{2M}^{(2l-k-1/2)}z)P_L(W_{2M}^{-(k+1/2)}z)\end{aligned} \tag{21}$$

for $1\le l\le M-1$. If we assume that the stopband attenuation of filter P_L is high enough so that the overlap among nonadjacent channel filters can be neglected, the only nonzero terms in (21) occur when $k=M-l, k=M-l-1$ in the second term, and $k=l, k=l-1$ in the third term, and hence

$$\begin{aligned}T_l(z)=\frac{1}{M}\{&P_L(-W_{2M}^{(l+1/2)}z)P_L(-W_{2M}^{(l-1/2)}z)\\ &\cdot[e^{j(\phi_{M-l}-\psi_{M-l})}+e^{j(\phi_{M-l-1}-\psi_{M-l-1})}]\\ &+P_L(W_{2M}^{(l+1/2)}z)P_L(W_{2M}^{(l-1/2)}z)\\ &\cdot[e^{-j(\phi_l-\psi_l)}+e^{-j(\phi_{l-1}-\psi_{l-1})}]\}.\end{aligned} \tag{22}$$

Substituting ϕ_l and ψ_l into (22), one can show that

$$T_l(z)=0 \qquad \text{for } 1\le l\le M-1$$

which implies that the aliasing terms are cancelled.

Under the assumption that the aliasing components are completely cancelled, the overall frequency response can now be expressed as

$$\begin{aligned}T_0(e^{j\omega})&=\frac{1}{M}\sum_{k=0}^{M-1}H_k(e^{j\omega})F_k(e^{j\omega})\\ &=\frac{1}{M}\sum_{k=0}^{M-1}e^{j(\phi_k+\psi_k)}P_L^2(W_{2M}^{(k+1/2)}e^{j\omega})\\ &\quad+e^{-j(\phi_k+\psi_k)}P_L^2(W_{2M}^{-(k+1/2)}e^{j\omega}).\end{aligned} \tag{23}$$

Substituting (19) into (23) and considering ω in the range $[-\pi/(2M), \pi/(2M)]$, we have

$$T_0(e^{j\omega}) \approx \frac{e^{-jk_d\omega}}{M}[|P_L(e^{j(\omega-\pi/2M)})|^2 + |P_L(e^{j(\omega+\pi/2M)})|^2]. \tag{24}$$

As in the design of conventional cosine-modulated QMF banks, if $|P_L(e^{j(\omega-\pi/2M)})|^2 + |P_L(e^{j(\omega+\pi/2M)})|^2$ is made sufficiently flat over $[-\pi/(2M), \pi/(2M)]$, then $|T_0(e^{j\omega})|$ will be flat for all frequencies. The perfect-reconstruction condition can be approximated by minimizing the error component

$$\begin{aligned} E_{L1} &= \int_{-\pi/(2M)}^{\pi/(2M)} |MT_0(e^{j\omega}) - e^{-jk_d\omega}|^2\, d\omega \\ &= \int_{-\pi/(2M)}^{\pi/(2M)} |e^{-jk_d\omega}[|P_L(e^{j(\omega-\pi/2M)})|^2 \\ &\quad + |P_L(e^{j(\omega+\pi/2M)})|^2] - e^{-jk_d\omega}|^2\, d\omega \\ &= \int_0^{\pi/M} |e^{-jk_d\omega}[|P_L(e^{j\omega})|^2 \\ &\quad + |P_L(e^{j(\omega-\pi/M)})|^2] - e^{-jk_d\omega}|^2\, d\omega \\ &= \int_0^{\pi/M} ||P_L(e^{j\omega})|^2 e^{-jk_d\omega} \\ &\quad + e^{-k_d\pi/M}|P_L(e^{j(\omega-\pi/M)})|^2 e^{-jk_d(\omega-\pi/M)} \\ &\quad - e^{-jk_d\omega}|^2\, d\omega \\ &= \int_0^{\pi/M} |P_L^2(e^{j\omega}) + e^{-jk_d\pi/M}P_L^2(e^{j(\omega-\pi/M)}) \\ &\quad - e^{-jk_d\omega}|^2\, d\omega. \end{aligned} \tag{25a}$$

Since the phase response of P_L is only approximately linear, both the phase and amplitude responses must be optimized, and hence, the above objective function includes both phase and magnitude error components. By also considering the stopband attenuation of filter P_L, the error component

$$E_{L2} = \int_{\omega_s}^{\pi} |P_L(e^{j\omega})|^2\, d\omega \tag{25b}$$

can be formed. A suitable objective function can now be constructed as

$$E_L = E_{L1} + \alpha E_{L2} \tag{26}$$

where α is a positive constant. To achieve the required design, the objective function in (26) is minimized with respect to the coefficients of P_L.

Having the coefficients of P_L, the impulse responses of the analysis filters H_k and the synthesis filters F_k can be obtained from (20) as

$$h_k(n) = 2p_L(n)\cos\left[(2k+1)\frac{\pi}{2M}\left(n - \frac{k_d}{2}\right) + \theta_k\right] \tag{27a}$$

$$f_k(n) = 2p_L(n)\cos\left[(2k+1)\frac{\pi}{2M}\left(n - \frac{k_d}{2}\right) - \theta_k\right] \tag{27b}$$

for $0 \le n \le N-1$ and $0 \le k \le M-1$, where $\theta_k = (2k+1)\pi/4$ and $p_L(n)$ is the impulse response of the prototype filter P_L.

On comparing (27) with (4), we observe that the filter bank proposed in Section III is a general version of the filter bank of Section II, which includes the latter filter bank as the *particular* case when filter P_L has a symmetrical impulse response, and $k_d = N-1$. It should also be emphasized that no constraint has been imposed on the filter length N and the reconstruction delay k_d of the cosine-modulated QMF bank in (27).

B. Design Method

Instead of minimizing the highly nonlinear objective function in (26) directly, an iterative procedure similar to that of Section II-B can be used in which the objective function is modified as

$$E'_L = E'_{L1} + \alpha E'_{L2} \tag{28a}$$

where

$$\begin{aligned} E'_{L1} = \sum_{0\le\omega\le\pi/M} &|P_L(e^{j\omega})Q_L(e^{j\omega}) \\ &+ e^{-jk_d\pi/M}P_L(e^{j(\omega-\pi/M)})Q_L(e^{j(\omega-\pi/M)}) \\ &- e^{-jk_d\omega}|^2 \end{aligned} \tag{28b}$$

$$E'_{L2} = \int_{\omega_s}^{\pi} |Q_L(e^{j\omega})|^2\, d\omega \tag{28c}$$

where Q_L is a lowpass FIR filter with a bandwidth $\pi/(2M)$, and the frequency responses of P_L and Q_L can be expressed as

$$\begin{aligned} P_L(e^{j\omega}) &= \boldsymbol{p}_L^T \boldsymbol{c}_L(\omega) \\ Q_L(e^{j\omega}) &= \boldsymbol{q}_L^T \boldsymbol{c}_L(\omega) \end{aligned}$$

where $\boldsymbol{c}_L(\omega) = [1\, e^{-j\omega} \cdots e^{-j(N-1)\omega}]^T$, and $\boldsymbol{p}_L = [p(0)\, p(1) \cdots p(N-1)]^T$, and $\boldsymbol{q}_L = [q(0)\, q(1) \cdots q(N-1)]^T$ are the coefficient vectors of filters P_L and Q_L, respectively.

We begin the iterative procedure by designing a filter P_L with group delay $k_d/2 < (N-1)/2$ using a least-squares design approach similar to that in [22] and write E'_L in (28a) as

$$E'_L = (\boldsymbol{U}\boldsymbol{q}_L - \boldsymbol{d}_L)^H(\boldsymbol{U}\boldsymbol{q}_L - \boldsymbol{d}_L) + \alpha \boldsymbol{q}_L^H \boldsymbol{U_s} \boldsymbol{q}_L \tag{29}$$

where $\boldsymbol{d}_L = [e^{-j\omega_{p1}k_d}\, e^{-j\omega_{p2}k_d} \cdots e^{-j\omega_{pk}k_d}]^T$, and superscript H denotes complex conjugate transposition. In this case, we have

$$\begin{aligned} \boldsymbol{U} &= \boldsymbol{H}(\boldsymbol{\Omega}_p)\boldsymbol{U_t}(\boldsymbol{\Omega}_p) + e^{-jk_d\pi/M}\boldsymbol{H}\left(\boldsymbol{\Omega}_p - \frac{\pi}{M}\right) \\ &\quad \cdot \boldsymbol{U_t}\left(\boldsymbol{\Omega}_p - \frac{\pi}{M}\right) \end{aligned} \tag{30a}$$

$$\boldsymbol{H}(\boldsymbol{\Omega}_p) = \mathrm{diag}[P_L(e^{j\omega_{p1}}), P_L(e^{j\omega_{p2}}), \cdots, P_L(e^{j\omega_{pk}})] \tag{30b}$$

$$\boldsymbol{U_t}(\Omega_p) = \begin{bmatrix} 1 & e^{-j\omega_{p1}} & \cdots & e^{-j\omega_{p1}(N-1)} \\ 1 & e^{-j\omega_{p2}} & \cdots & e^{-j\omega_{p2}(N-1)} \\ \vdots & \vdots & & \vdots \\ 1 & e^{-j\omega_{pk}} & \cdots & e^{-j\omega_{pk}(N-1)} \end{bmatrix} \tag{30c}$$

and $\boldsymbol{U_s}$ is given by (30d), which appears at the bottom of the next page. As E'_L in (29) is a quadratic function in $\boldsymbol{q}_L$ with $[\mathrm{Re}(\boldsymbol{U}^H\boldsymbol{U}) + \alpha\boldsymbol{U_s}] > 0$, it has the unique global minimum point given by

$$\boldsymbol{q}_L = [\mathrm{Re}(\boldsymbol{U}^H\boldsymbol{U}) + \alpha\boldsymbol{U_s}]^{-1} \cdot \mathrm{Re}(\boldsymbol{U}^H\boldsymbol{d}_L) \tag{31}$$

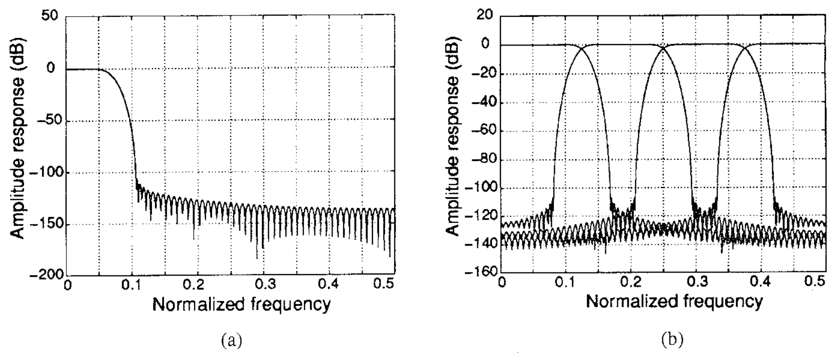

Fig. 2. Example 1: (a) Amplitude response of the prototype filter; (b) amplitude responses of the analysis filters.

where Re[·] is the real part of [·]. Having obtained $\boldsymbol{q}_L$, a linear formula can be used to update $\boldsymbol{p}_L$ as

$$\boldsymbol{p}_L := (1-\tau)\boldsymbol{p}_L + \tau \boldsymbol{q}_L. \tag{32}$$

The procedure is repeated until $\|\boldsymbol{p}_L - \boldsymbol{q}_L\|_2$ is less than a prescribed tolerance. The iterative algorithm for the design of cosine-modulated QMF banks with low reconstruction delays can now be summarized in terms of the following simple steps.

Algorithm 2

Step 1: Use a least-squares approach to design a lowpass FIR filter of length N with stopband edge ω_s and group delay $k_d/2$, and use the coefficient vector of the filter obtained to initialize $\boldsymbol{p}_L$.

Step 2: Use (30d) to compute matrix $\boldsymbol{U}_s$.

Step 3: Form matrix $\boldsymbol{U}$ and vector $\boldsymbol{q}_L$ using (30a) and (31), respectively.

Step 4: If $\|\boldsymbol{p}_L - \boldsymbol{q}_L\|_2 < \epsilon$, where ϵ is a prescribed tolerance, output $\boldsymbol{p}_L$ as the desired result and stop; otherwise, update $\boldsymbol{p}_L$ using (32) with τ in the range $0 < \tau < 1$, say, $\tau = 0.5$, and repeat from Step 3.

In our experiments, we noticed that undesirable artifacts can sometimes occur in the amplitude responses of the analysis and synthesis filters when the reconstruction delay is low. Such artifacts have been observed as well by other researchers when designing low-delay two-channel filter banks [23], [24] and multichannel cosine-modulated filter banks [17], [20]. In the multichannel case, artifacts can occur in the transition band of the prototype filter P_L when the group delay is low if there is no constraint on its transition band. These artifacts then lead to artifacts in the amplitude responses of the analysis and synthesis filters. An effective treatment of this problem is to modify the objective function in (28a) to include an additional term $\alpha_1 E'_{L3}$, i.e.,

$$E'_L = E'_{L1} + \alpha E'_{L2} + \alpha_1 E'_{L3} \tag{33}$$

where

$$\alpha_1 E'_{L3} = \alpha_1 \int_{\omega_{t1}}^{\omega_{t2}} |Q_L(e^{j\omega}) - e^{-jk_d\omega/2}|^2 \, d\omega \tag{34}$$

and $[\omega_{t1}, \omega_{t2}]$ is an interval in the transition region where the artifacts occur. It can be readily shown that the objective function in (33) can be written as

$$\begin{aligned} E'_L = {} & (\boldsymbol{U}\boldsymbol{q}_L - \boldsymbol{d}_L)^H(\boldsymbol{U}\boldsymbol{q}_L - \boldsymbol{d}_L) + \alpha \boldsymbol{q}_L^H \boldsymbol{U_s} \boldsymbol{q}_L \\ & + \alpha_1(\boldsymbol{q}_L^T \boldsymbol{U}_a \boldsymbol{q}_L - 2\boldsymbol{b}^T \boldsymbol{q}_L + \omega_{t2} - \omega_{t1}) \end{aligned} \tag{35}$$

where $\boldsymbol{U}$ and $\boldsymbol{U}_s$ are given by (30a) and (30d), respectively, and $\boldsymbol{U}_a$ is given by the expression at the bottom of the next page. The global minimum point of E'_L in each step of the iterative algorithm can now be obtained as

$$\boldsymbol{q}_L = [\mathrm{Re}(\boldsymbol{U}^H\boldsymbol{U}) + \alpha \boldsymbol{U_s} + \alpha_1 \boldsymbol{U}_a]^{-1} \cdot [\mathrm{Re}(\boldsymbol{U}^H \boldsymbol{d}_L) + \alpha_1 \boldsymbol{b}]. \tag{36}$$

The proposed low-delay cosine-modulated QMF bank can be implemented by the efficient polyphase implementation using the discrete Fourier transform (DFT) as described in [17]. The numbers of multiplications and additions per output sample are comparable with those required by the cosine-modulated filter bank in [19], which is based on the extended lapped transformation.

IV. Design Examples

In this section, we apply the iterative design algorithms described in Sections II and III to several examples. All the designs were carried out by running MATLAB programs on a

$$\boldsymbol{U_s} = \mathrm{Re}\int_{\omega_s}^{\pi} \boldsymbol{c}_L(\omega)\boldsymbol{c}_L^H(\omega)\, d\omega = \begin{bmatrix} \pi - \omega_s & -\sin\omega_s & -\frac{1}{2}\sin 2\omega_s & \cdots & -\frac{1}{N-1}\sin(N-1)\omega_s \\ -\sin\omega_s & \pi - \omega_s & -\sin\omega_s & \cdots & -\frac{1}{N-2}\sin(N-2)\omega_s \\ \vdots & \vdots & & & \vdots \\ -\frac{1}{N-1}\sin(N-1)\omega_s & \cdots & \cdots & \cdots & \pi - \omega_s \end{bmatrix} \tag{30d}$$

Sun SPARC workstation. The performance of the filter banks designed are evaluated in terms of computational efficiency, reconstruction error, and implementation considerations. The performance criteria are as follows:

- iterations used in the design (IN)
- flops used in millions of floating point operations (MFLOPS)
- the maximum reconstruction error

$$E_r = \max_{\omega} |[|MT_0(e^{j\omega})| - 1]|$$

- the aliasing error

$$E_a = \max_{\omega} E(\omega)$$

where

$$E(\omega) = \frac{1}{M}\left[\sum_{l=1}^{M-1} |T_l(e^{j\omega})|^2\right]^{1/2}$$

$$T_l(e^{j\omega}) = \sum_{k=0}^{M-1} H_k(e^{j(\omega - 2\pi l/M)})F_k(e^{j\omega})$$

- the signal-to-noise ratio (SNR)

$$\begin{aligned}\text{SNR} &= 10\log_{10}\left(\frac{\text{energy of input signal}}{\text{energy of the reconstruction error}}\right)\\ &= 10\log_{10}\left\{\frac{\sum x^2(n)}{\sum[x(n) - \hat{x}(n+k_d)]^2}\right\}\end{aligned}$$

where k_d is the reconstruction delay

- the number of multiplications per output sample in the implementation (MPU) [17]

$$\text{MPU} = 12 + 2N/M + 4\log_2(2M)$$

- the number of additions per output sample in the implementation (APU) [17]

$$\text{APU} = 4 + 2N/M + 4\log_2(2M).$$

To calculate the SNR, the input signal $x(n)$ was chosen to be a random signal whose amplitude is uniformly distributed between 0 and 1. The signal length was 1000.

A. Conventional Filter Banks

Algorithm 1 was used to design three cosine-modulated QMF banks as follows:

Example 1: In this example, a four-band cosine-modulated QMF bank satisfying the specifications

$$M = 4, N = 112, \alpha = 200, \omega_s = 0.2109\pi, \tau = 0.5, \epsilon = 10^{-4}$$

was designed. The initial point $\boldsymbol{p}$ in Step 1 of Algorithm 1 was the coefficient vector of a lowpass FIR filter designed by using the window method. The sampling grid contained 200 sampling points. The results obtained are summarized in Table I. Fig. 2(a) and (b) show the amplitude responses of the prototype filter and the analysis filters, respectively. To demonstrate the design efficiency of the iterative algorithm, the quasi-Newton method using the Broyden-Fletcher-Goldfard-Shanno (BFGS) formula for updating the approximation of the inverse Hessian matrix of the objective function [25] was used to design the same filter bank with the same initial point and sampling points. The quasi-Newton method completed the design with about 502 MFLOPS, which is almost 60 times that used by the iterative algorithm.

Example 2: A 16-channel cosine-modulated QMF bank was designed satisfying the specifications

$$\begin{aligned}M &= 16, N = 386, \alpha = 100,\\ \omega_s &= 0.0567\pi, \tau = 0.5, \epsilon = 10^{-4}.\end{aligned}$$

The results obtained are listed in Table I. Graphical displays for the filter bank in Example 2 are shown in Fig. 3(a)–(d). Fig. 3(a) illustrates the amplitude responses of the analysis filters. Fig. 3(b) shows the overall amplitude response of the filter bank, i.e., $|MT_0(e^{j\omega})|$, and Fig. 3(c) shows the aliasing error $E(\omega)$. Fig. 3(d) depicts the amplitude spectrums of the input signal and the reconstruction error. From Table I and the figures, it can be observed that the iterative algorithm leads to analysis and synthesis filters with a high stopband attenuation ($\geq$ 120 dB) and low overall distortion and aliasing

$$\boldsymbol{U}_a = \begin{bmatrix} \omega_{t2} - \omega_{t1} & \phi(\omega_{t2}, \omega_{t1}, 1) & \cdots & \phi(\omega_{t2}, \omega_{t1}, N-1) \\ \phi(\omega_{t2}, \omega_{t1}, 1) & \omega_{t2} - \omega_{t1} & & \vdots \\ \vdots & \vdots & & \\ \phi(\omega_{t2}, \omega_{t1}, N-1) & \cdots & \cdots & \omega_{t2} - \omega_{t1} \end{bmatrix}$$

$$\phi(\omega_{t2}, \omega_{t1}, k) = \frac{1}{k}[\sin k\omega_{t2} - \sin k\omega_{t1}]$$

$$\boldsymbol{b} = \text{Re}\int_{\omega_{t1}}^{\omega_{t2}} \boldsymbol{c}_L(\omega)e^{jk_d\omega/2}\, d\omega = \begin{bmatrix} \frac{2}{k_d}\left[\sin\left(\frac{k_d\omega_{t2}}{2}\right) - \sin\left(\frac{k_d\omega_{t1}}{2}\right)\right] \\ \frac{2}{k_d - 2}\left\{\sin\left[\left(\frac{k_d}{2} - 1\right)\omega_{t2}\right] - \sin\left[\left(\frac{k_d}{2} - 1\right)\omega_{t1}\right]\right\} \\ \vdots \\ \frac{2}{k_d - 2N + 2}\left\{\sin\left[\left(\frac{k_d}{2} - N + 1\right)\omega_{t2}\right] - \sin\left[\left(\frac{k_d}{2} - N + 1\right)\omega_{t1}\right]\right\} \end{bmatrix}$$

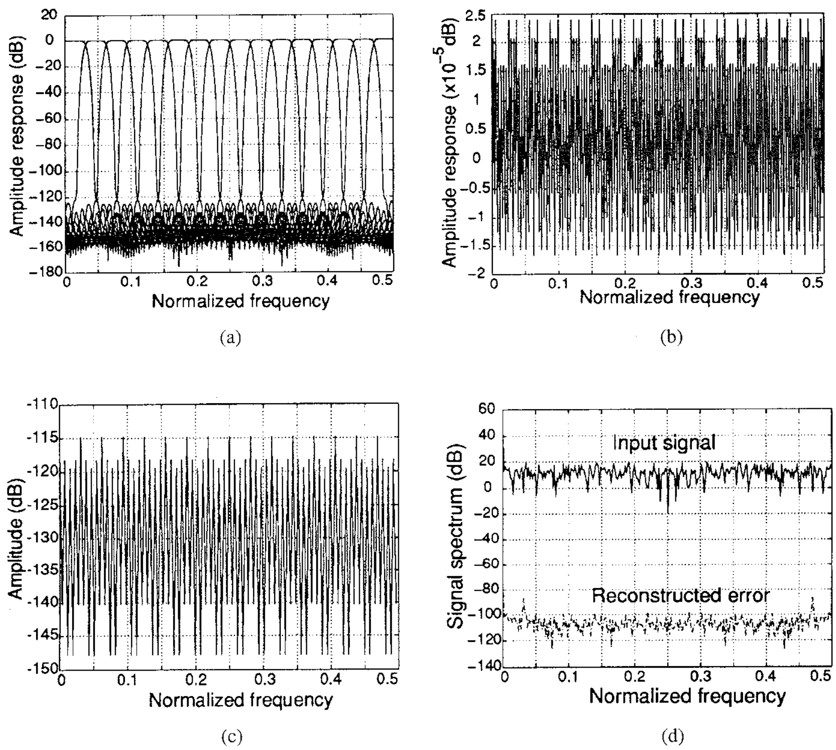

Fig. 3. Example 2: (a) Amplitude responses of the analysis filters; (b) amplitude response of the filter bank; (c) plot of the aliasing error $E(\omega)$; (d) spectrums of the input signal and the reconstruction error.

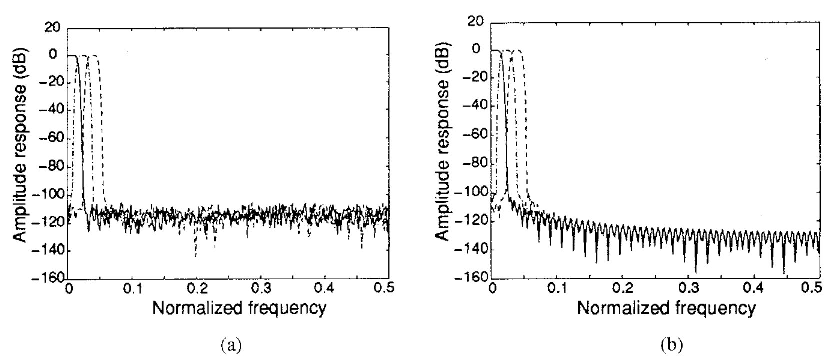

Fig. 4. Example 3: (a) Amplitude responses of the analysis filters in the current MPEG standard; (b) amplitude responses of the analysis filters designed.

levels (≈ -100 dB). Such filter specifications were previously achieved with a constrained optimization method [16]. Using the algorithm in [16], the reconstruction error E_r is of the order of 10^{-13}, whereas in our approach, it is of the order of 10^{-6}. However, since the aliasing errors E_a achieved by both algorithms are of the order of 10^{-6} (-120 dB), in both cases the output signals $\hat{x}(n)$ approximate the input signals $x(n)$ with about -100 dB reconstruction error. This is evident from the large difference between the amplitude spectrums of the input and the reconstructed error signals as depicted in Fig. 3(d).

Example 3: A 32-band cosine-modulated QMF bank satisfying the specifications

$$M = 32, N = 513, \alpha = 100,$$
$$\omega_s = 0.0315\pi, \tau = 0.5, \epsilon = 10^{-4}$$

was designed. The results obtained are given in Table I. Fig. 4(a) shows the amplitude responses of the first three analysis filters obtained in the design. For comparison, the amplitude responses of the first three analysis filters adopted in the current Moving Picture Expert Group (MPEG) standard on audio compression [26] are depicted in Fig. 4(b). As can be seen from Table I, our design has an SNR of 97.1 dB as opposed to 84.3 dB for the MPEG filter bank with the same test signal. From Fig. 4, our design shows improved stopband attenuation with comparable transition bands with those in the MPEG filter bank.

B. Filter Banks with Low Reconstruction Delays

Algorithm 2 was used to design three low-delay cosine-modulated QMF banks.

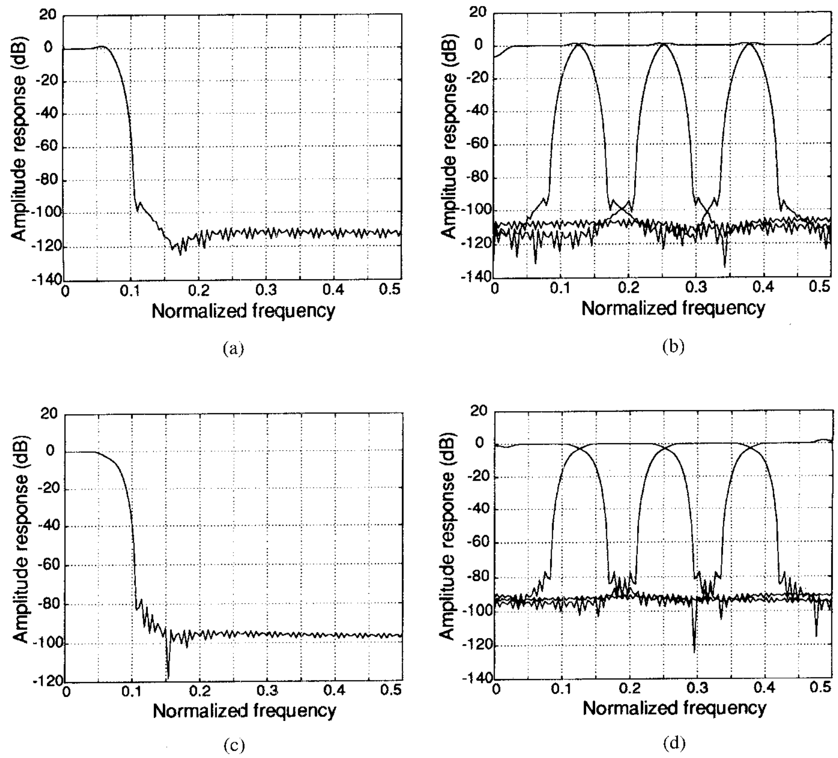

Fig. 5. Example 4: (a) Prototype filter with artifacts; (b) analysis filters with artifacts; (c) prototype filter with reduced artifacts; (d) analysis filters with reduced artifacts.

Example 4: This example demonstrates that artifacts can occur when designing a low-delay cosine-modulated QMF bank and that it is possible to reduce them. First, a four-channel filter bank was designed with $N = 112, k_d = 55$, and no constraint was applied to the transition band of the prototype filter. Fig. 5(a) and (b) show the amplitude responses of the prototype filter P_L obtained and the analysis filters, respectively. It can be observed that there is a 'bump' in the transition band of P_L, which, in turn, leads to the artifacts in the amplitude response of each analysis and synthesis filter. To reduce the artifacts, the modified objective function in (33) was used to design a filter bank satisfying the specifications

$$\begin{aligned} M &= 4, N = 112, k_d = 55, \alpha = 10, \\ \alpha_1 &= 10^{-3}, \omega_s = 0.2078\pi \\ \tau &= 0.5, \omega_{t1} = 0.1234\pi, \omega_{t2} = 0.1266\pi, \epsilon = 10^{-3}. \end{aligned}$$

The results obtained are summarized in Table II. Fig. 5(c) and (d) show the amplitude responses of the prototype filter P_L and the analysis filters, respectively. Comparing them with Fig. 5(a) and (b), we note that the artifacts are reduced significantly. On comparing the filter bank designed in this example with that in Example 1, we observe that the reconstruction delay in the present design is only about 50% of that in Example 1. However, this low delay is achieved at the cost of reduced stopband attenuation and SNR ratio. This was found to be the case in a number of designs, and as a consequence, we believe that the designer can trade off stopband attenuation and reconstruction error for a lower reconstruction delay.

TABLE I
RESULTS FOR EXAMPLES 1, 2, AND 3

	Example 1	Example 2	Example 3
IN	12	14	11
MFLOPS	8.66	219	523
E_r	3.2594×10^{-6}	2.7563×10^{-6}	2.9941×10^{-6}
E_a	3.2178×10^{-7}	2.5814×10^{-7}	5.7532×10^{-7}
SNR (dB)	111.5	115.7	97.1
MPU	80	82	68
APU	72	74	60

Example 5: In this example, an eight-band low-delay cosine-modulated QMF bank satisfying the specifications

$$\begin{aligned} M &= 8, N = 132, k_d = 65, \alpha = 20, \\ \alpha_1 &= 10^{-3}, \omega_s = 0.1357\pi \\ \tau &= 0.5, \omega_{t1} = 0.0561\pi, \omega_{t2} = 0.0609\pi, \epsilon = 10^{-3} \end{aligned}$$

was designed. The results are listed in Table II. Fig. 6(a) shows the amplitude response of the prototype filter, and Fig. 6(b) shows its group delay in the passband and transition band. Fig. 6(c) and (d) shows the amplitude response of the analysis filters obtained and the group delay of the filter bank. For comparison, Algorithm 1 was used to design a conventional cosine-modulated QMF bank with a filter length of 66 and a reconstruction delay of 65 sampling periods.

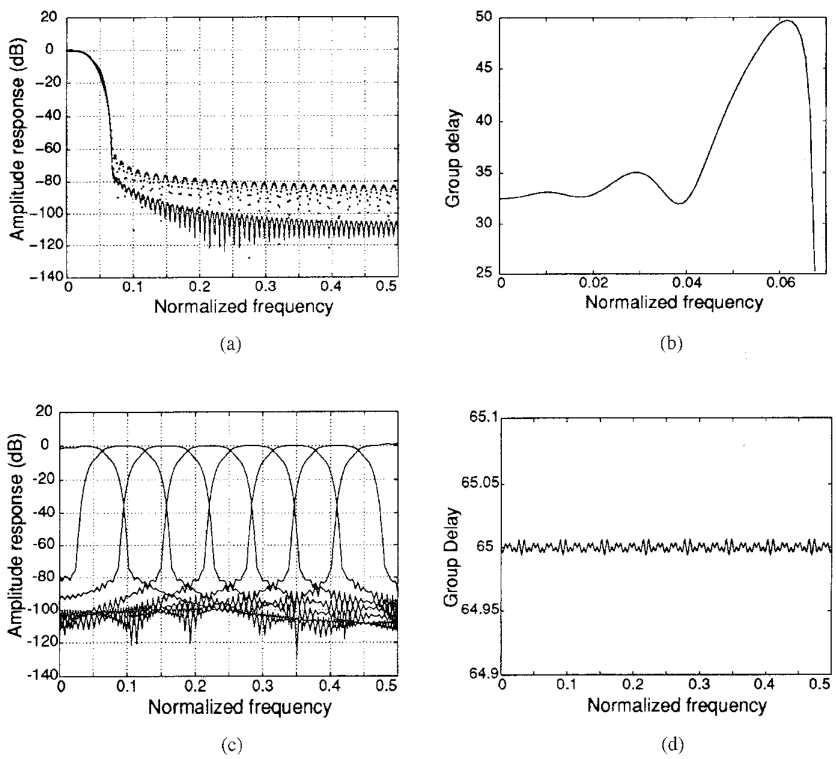

Fig. 6. Example 5: (a) Amplitude responses of prototype filters; (b) group delay of the prototype filter (low-delay); (c) amplitude responses of analysis filters (low-delay); (d) group delay of the filter bank (low-delay).

The SNR achieved by this filter bank is 62 dB, and the amplitude response of its prototype filter is also shown in Fig. 6(a). It is observed that with the same reconstruction delay, the low-delay cosine-modulated QMF bank shows improved performance over the conventional cosine-modulated QMF bank. From Fig. 6(b), it can be noticed that in the passband of the prototype filter, linear phase is well approximated, and the phase distortion in its stopband can be neglected due to very small amplitude response. As mentioned in Section III, in the low-delay QMF bank proposed, both the phase distortion and the amplitude distortion are minimized. Fig. 6(d) shows that the phase distortion of the filter bank obtained is small.

Example 6: A 32-band QMF bank satisfying the specifications

$$M = 32, N = 513, k_d = 255, \alpha = 5000,$$
$$\omega_s = 0.0347\pi, \tau = 0.5, \epsilon = 10^{-3}$$

was designed. The results are illustrated in Table II, and Fig. 7(a) shows the amplitude responses of the analysis filters. Compared with the current MPEG filter bank, the reconstruction delay of the filter bank designed is reduced by half. In addition, this low-delay filter bank can be implemented by a polyphase structure similar to that described in [26]. As a performance test, a ramp signal was used as the input. The input, the outputs from the low-delay QMF bank designed, and the current MPEG QMF bank are depicted in Fig. 7(b). The figure shows that, in agreement with the design specifications, our design only takes about 50% of the time required by the current MPEG filter bank to reconstruct the input signal.

TABLE II
RESULTS FOR EXAMPLES 4, 5, AND 6

	Example 4	Example 5	Example 6
k_d	55	65	255
IN	11	13	7
E_r	3.9808×10^{-5}	1.8041×10^{-4}	7.1657×10^{-5}
E_a	5.1584×10^{-6}	5.0333×10^{-5}	4.6497×10^{-6}
SNR (dB)	88.3	82.8	90.4
MPU	80	62	68
APU	72	54	60

V. CONCLUSION

An iterative algorithm for the design of conventional cosine-modulated QMF banks has been proposed. The algorithm is very efficient and can design filter banks with high stopband attenuation and low aliasing and amplitude distortions. Although a rigorous proof on the convergence of the algorithm is not available at this time, the algorithm converged in all the design examples attempted. A general version of the algorithm has then been developed, which can be used to design low-delay cosine-modulated QMF banks. This algorithm is based on a weighted objective function that depends on the error between the actual frequency response and that of a linear-phase ideal filter. Artifacts that can occur in the amplitude responses of the analysis and synthesis filters when designing low-delay filter banks can be reduced significantly by simply adding one more

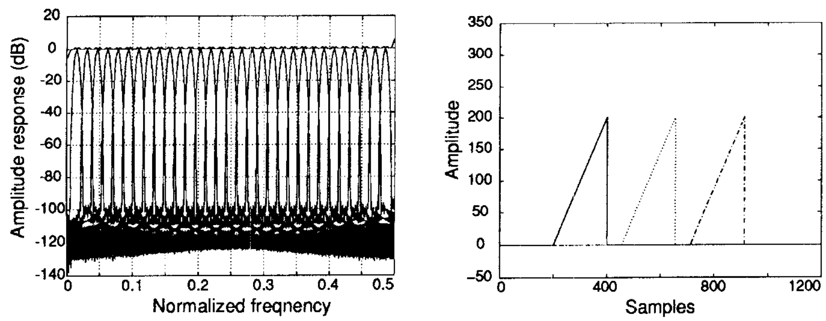

Fig. 7. Example 6: (a) Analysis filters; (b) a ramp input and outputs from the low-delay QMF bank and the current MPEG QMF bank.

error component to the objective function. The two algorithms have been illustrated by designing several filter banks, and the designs obtained have been compared with corresponding designs obtained by using some other known methods.

REFERENCES

[1] R. E. Crochiere, S. A. Webber, and J. L. Flanagan, "Digital coding of speech in subbands," *Bell Sys. Tech. J.*, vol. 55, pp. 1069–1085, Oct. 1976.
[2] D. Esteban and C. Galand, "Application of quadrature mirror filter to split-band voice coding schemes," in *Proc. IEEE Int. Conf. Acoust., Speech, Signal Processing*, May 1977, pp. 191–195.
[3] J. W. Woods and S. D. O'Neil, "Subband coding of images," *IEEE Trans. Acoust., Speech, Signal Processing*, vol. ASSP-34, pp. 1278–1288, Oct. 1986.
[4] J. W. Woods, Ed., *Subband Image Coding*. Boston: Kluwer, 1991.
[5] M. Rabbani and P. W. Jones, *Digital Image Compression Techniques*. Bellingham, 1991.
[6] J. D. Johnston, "A filter family designed for use in quadrature mirror filter banks," in *Proc. IEEE Int. Conf. Acoust., Speech, Signal Processing*, Mar. 1980, pp. 291–294.
[7] R. E. Crochiere and L. R. Rabiner, *Multirate Digital Signal Processing*. Englewood Cliffs, NJ: Prentice-Hall, 1983.
[8] V. K. Jain and R. E. Crochiere, "Quadrature mirror filter design in the time domain," *IEEE Trans. Acoust., Speech, Signal Processing*, vol. ASSP-32, pp. 353–361, Apr. 1984.
[9] P. P. Vaidyanathan, "Multirate digital filters, filter banks, polyphase network, and applications: A tutorial," *Proc. IEEE*, vol. 78, pp. 56–93, Jan. 1990.
[10] C.-K. Chen and J.-H. Lee, "Design of quadrature mirror filters with linear phase in the frequency domain," *IEEE Trans. Circuits Syst.*, vol. 39, pp. 593–605, Sept. 1992.
[11] P. P. Vaidyanathan, "Theory and design of M-channel maximally decimated quadrature mirror filters with arbitrary M, having perfect reconstruction property," *IEEE Trans. Acoust., Speech, Signal Processing*, vol. ASSP-35, pp. 476–492, Apr. 1987.
[12] J. H. Rothweiler, "Polyphase quadrature filters—A new subband coding technique," in *Proc. IEEE Int. Conf. ASSP*, Boston, MA, 1983, pp. 1280–1283.
[13] J. Mason and Z. Picel, "Flexible design of computationally efficient nearly perfect QMF filter banks," in *Proc. IEEE Int. Conf. ASSP*, Tampa, FL, Mar. 1985, pp. 14.7.1–14.7.4.
[14] P. P. Vaidyanathan, *Multirate Systems and Filter Banks*. Englewood Cliffs, NJ: Prentice-Hall, 1993.
[15] R. D. Koilpillai and P. P. Vaidyanathan, "A spectral factorization approach to pseudo-QMF design," in *Proc. Int. Symp. Circuits Syst.*, Singapore, May 1991.
[16] T. Q. Nguyen, "Near-perfect-reconstruction pseudo-QMF banks," *IEEE Trans. Signal Processing*, vol. 42, pp. 65–75, Jan. 1994.
[17] K. Nayebi, T. P. Barnwell, III, and M. J. T. Smith, "On the design of FIR analysis-synthesis filter banks with high computational efficiency," *IEEE Trans. Signal Processing*, vol. 42, pp. 825–833, Apr. 1994.
[18] R. D. Koilpillai and P. P. Vaidyanathan, "Cosine-modulated QMF banks satisfying perfect reconstruction," *IEEE Trans. Signal Processing*, vol. 40, pp. 770–783, Apr. 1992.
[19] H. S. Malvar, "Extended lapped transforms: properties, applications, and fast algorithms," *IEEE Trans. Signal Processing*, vol. 40, pp. 2703–2714, Nov. 1992.
[20] T. Q. Nguyen, "A class of generalized cosine-modulated filter bank," in *Proc. Int. Symp. Circuits Syst.*, San Diego, May 1992, pp. 943–946.
[21] A. Antoniou, *Digital Filters: Analysis, Design, and Applications*. New York: McGraw-Hill, 1993, 2nd ed.
[22] S. Sunder and R. P. Ramachandran, "A least-squares design of nonrecursive filters satisfying prescribed magnitude and phase specifications," *IEEE Int. Symp. Circuits Syst.*, Chicago, May 1993, pp. 335–338.
[23] K. Nayebi, T. P. Barnwell, III, and M. J. T. Smith, "Time-domain filter bank analysis: A new design theory," *IEEE Trans. Signal Processing*, vol. 40, pp. 1412–1429, June 1992.
[24] ——, "Low delay QMF banks: Design and evaluation," *IEEE Trans. Signal Processing*, vol. 42, pp. 24–31, Jan. 1994.
[25] R. Fletcher, *Practical Methods of Optimization*. New York: Wiley, 1987, 2nd ed.
[26] ISO/IEC 11172-3, "Coding of moving pictures and associated audio for digital storage at up to about 1.5 Mbit/s—Part 3: Audio," ISO/IEC, Switzerland, Aug. 1993.

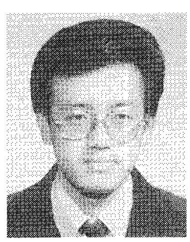

Hua Xu (S'91) received the B.Eng. degree from Tsinghua University, Beijing, China, in 1988, the M.Eng. degree from Southeast University, Nanjing, China, in 1991, and the Ph.D degree from University of Victoria, Victoria, Canada, in 1995, all in electrical engineering.

From September 1991 to August 1995, he was with the Department of Electrical and Computer Engineering, University of Victoria, working as a research assistant. He joined INRS Telecommunications, Montreal, Canada, as a research associate in September 1995.

His research interests include multirate signal processing, filter bank design, speech coding, and audio and video processing and transmission.

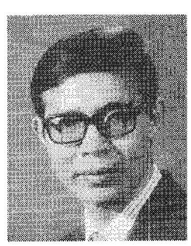

Wu-Sheng Lu (S'81–M'85–SM'90) received the B.S. degree in mathematics from Fudan University, China, in 1964 and the M.S. degree in electrical engineering and the Ph.D. degree in control science from the University of Minnesota, Minneapolis, in 1983 and 1984, respectively.

He was a postdoctoral fellow at the University of Victoria, Victoria, Canada, in 1985 and held a visiting assistant professorship at the University of Minnesota in 1986. Since 1987, he has been with the University of Victoria, where he is currently Professor. His teaching and research interests are in the areas of digital signal processing and robotics. He is the co-author, with A. Antoniou, of *Two-Dimensional Digital Filters* (New York: Marcel Dekker, 1992). He served as Associate Editor of the *Canadian Journal of Electrical and Computer Engineering* in 1989 and was Editor of the same journal from 1990 to 1992. He was an Associate Editor of the IEEE TRANSACTIONS ON CIRCUITS AND SYSTEMS–Part II from 1993 to 1995.

Andreas Antoniou (F'82) received the B.Sc. (Eng.) and Ph.D. degrees in electrical engineering from London University, London, Canada, in 1963 and 1966, respectively.

From 1966 to 1969, he was Senior Scientific Officer at the Post Office Research Department, London, Canada, and from 1969 to 1970, he was a member of the Scientific Staff at the R&D Laboratories of Northern Electric Company Ltd., Ottawa, Canada. From 1970 to 1983, he served in the Department of Electrical and Computer Engineering, Concordia University, Montreal, Canada, as Professor from June 1973 and as Chairman from December 1977. He served as founding Chairman of the Department of Electrical and Computer Engineering, University of Victoria, Victoria, Canada, from 1983 to 1990 and is now Professor in the same department. His teaching and research interests are in the areas of electronics, network synthesis, digital system design, active and digital filters, and digital signal processing. He has published extensively in these areas. He is the author of *Digital Filters: Analysis, Design, and Applications* (New York: McGraw-Hill) and the co-author, with W.-S. Lu, of *Two-Dimensional Digital Filters* (New York: Marcel Dekker).

Dr. Antoniou is a Member of the Association of Professional Engineers and Geoscientists of British Columbia and a Fellow of the Institution of Electrical Engineers. He was elected Fellow of the Institute of Electrical and Electronics Engineers for contributions to active and digital filters and to electrical engineering education. He served as Associate Editor of the IEEE TRANSACTIONS ON CIRCUITS AND SYSTEMS from June 1983 to May 1985 and as Editor of the same TRANSACTIONS from June 1985 to May 1987. He is currenlly serving as a member of the Board of Governors of the Circuits and Systems Society. One of his papers on gyrator circuits was awarded the Ambrose Fleming Premium by the Institution of Electrical Engineers of the UK.